Crystalline and Solution Phases of *N*,*N*-Dimethylethylenediamine Complexed with Lithium Triflate and Sodium Triflate: Intramolecular and Intermolecular Hydrogen Bonding

Nathalie M. Rocher, Roger Frech,* and Douglas R. Powell

Department of Chemistry and Biochemistry, University of Oklahoma, Norman, Oklahoma 73019

Received: February 22, 2006; In Final Form: May 25, 2006

Infrared and Raman spectroscopy were used to study hydrogen-bonding interactions and the cation coordination effect in solutions of *N*,*N*-dimethylethylenediamine (DMEDA) with lithium triflate (LiTf) and sodium triflate (NaTf). A comparison of pure DMEDA with DMEDA dissolved in carbon tetrachloride enabled the separation of the relative contributions of intermolecular and intramolecular hydrogen-bonding interactions to the N−H stretching frequencies. The addition of LiTf and NaTf to DMEDA shifts the N−H stretching frequencies through two competing effects: the cation coordination effect lowers the frequencies, while the disruption of the hydrogen-bonding interactions increases the frequencies. These two effects were distinguished in a study of the concentration dependence of both salts dissolved in DMEDA; the differentiation was based on the difference in the spectral sensitivities of the symmetric and the antisymmetric stretch in both the Raman and infrared spectra. During this study, DMEDA−LiTf and DMEDA−NaTf crystals were discovered, and their structures were solved by X-ray diffraction techniques. The analysis of the vibrational spectra of these crystals was greatly enhanced by unambiguous knowledge of the structural details of cation−molecule and anion−cation interactions. These structure−spectra correlations were used to complement analogous spectroscopic studies in the solution phases. Analysis of spectral regions in both crystalline and solution phases particularly sensitive to the nature and strength of cation−molecule interactions clearly established that the interaction of the lithium ion with the nitrogen atoms of DMEDA was stronger than the sodium ion−DMEDA interaction, as expected from charge density arguments.

1. Introduction

The study of polymer electrolytes for lithium batteries has been ongoing for the past 25 years, driven by the need to develop new polymer electrolytes with room-temperature conductivities on the order of 10^{-4} S cm^{-1}. Understanding the ionic conduction mechanisms in a polymer matrix at the molecular level is essential to improve the ionic conductivity of polymer electrolytes. Ion−ion interactions[1,2] and ion−polymer interactions[3,4] have been shown to be important factors controlling the ionic conductivity. These interactions affect the local structure of a polymer electrolyte through the formation of ionically associated species[5−8] and changes in the polymer backbone conformation.[9,10] It is possible to better understand these interactions in a polymer electrolyte by studying small molecules that structurally mimic small regions of a polymer.[11−14] Because the complexity of polymer electrolytes makes them difficult to study at a molecular level, these model compounds can provide significant insight into the local structures and structural changes accompanying the addition of a salt to a host polymer to form a polymer electrolyte.

In this study, we investigate complexes of *N*,*N*-dimethylethylenediamine (DMEDA) with lithium trifluoromethane sulfonate (LiTf) and sodium trifluoromethane sulfonate (NaTf). DMEDA is a small molecule that has a primary amine group and a tertiary amine group connected by an ethylene unit. DMEDA resembles small segments of high molecular weight branched poly(ethylenimine) (BPEI) and can be used to model the predominant interactions in the polymer electrolyte. BPEI is an amorphous polymer with primary, secondary, and tertiary amine groups in a molar ratio of 25:50:25, respectively,[15,16] and has been previously investigated as a potential host for polymer electrolytes.[17,18] Comparisons of IR and Raman spectra of DMEDA and BPEI and the corresponding salt systems show striking similarities; however, a detailed comparative study will be reported in a subsequent paper.

This study of DMEDA and DMEDA−salt systems is of fundamental interest in its own right, since it focuses on the vibrational behavior of the NH_2 group undergoing a variety of interactions. DMEDA is a complex molecule whose ion-coordinating sites can participate in intermolecular hydrogen bonds. Moreover, the architecture of the molecule allows for a stable conformation, leading to intramolecular hydrogen-bonding interactions. In this work, infrared and Raman spectroscopy of the NH stretching region have been the primary tools to analyze cation−molecule interactions. The addition of salt disturbs the NH_2 vibrations, not only through the coordination effect of the cation, but also through concurrent changes in the hydrogen-bonding environment. Subtle shifts of the NH_2 stretching modes allowed for separation of these effects to some degree. Furthermore, intermolecular and intramolecular hydrogen-bonded populations were identified. Although this work has technological applications related to lithium battery technology, it also presents a significant contribution to the area of coordination chemistry.

During the initial phase of this study, DMEDA−NaTf and DMEDA−LiTf crystals were isolated, and their structures were solved. Unambiguous knowledge of local structures present in salt complexes of DMEDA−LiTf and DMEDA−NaTf allows a more precise set of spectral−(local) structural correlations to

* Corresponding author. E-mail: rfrech@ou.edu. Tel: 405-325-3831. Fax: 405-325-6111.

10.1021/jp061143w CCC: $33.50
Published on Web 07/19/2006

be developed. These correlations can be used with some degree of confidence to study interactions in salt complexes with BPEI. This paper describes the characterization of the crystalline and solution phases of DMEDA−LiTf and DMEDA−NaTf systems using X-ray diffraction, differential scanning calorimetry (DSC), Fourier transform infrared (FT-IR), and Raman spectroscopy. Knowledge of the DMEDA−LiTf and DMEDA−NaTf crystal structures is also used to further our understanding of the coordination environment of the cation and anion in the DMEDA solution phases.

2. Experimental Section

DMEDA, LiTf, and NaTf were obtained from Aldrich. The salts were dried under vacuum at 120 °C for 48 h before use. The chemicals were stored and used in a dry argon atmosphere glovebox (VAC; ≤1 ppm H_2O) at room temperature. The DMEDA−salt solutions were prepared by mixing weighed amounts of salt and solvents. The solutions were stirred for a minimum of 24 h before use. The compositions of the samples are reported as a nitrogen to cation molar ratio ($N:M^+$). The DMEDA−LiTf and DMEDA−NaTf crystals formed by slow evaporation of solutions of various concentrations in the glovebox. The DMEDA−LiTf and the DMEDA−NaTf crystals were clear thin plates that formed first out of the highly concentrated solutions (3:1). In both systems, a thin clear "crust" appeared at the surface of the solution after a couple of months. A few months later, thin crystalline plates were floating in the solution. The crystals were then placed in X-ray oil in the glovebox to proceed with the X-ray measurements.

Single crystals for X-ray analysis were isolated from the 3:1 DMEDA−LiTf and DMEDA−NaTf solutions. The data were collected on a Bruker Apex diffractometer using Mo Kα radiation ($\lambda = 0.71073$ Å). The structures were solved by the direct method using the SHELXTL system, and refined by full-matrix least squares on F^2 using all reflections. All non-hydrogen atoms were refined anisotropically. All hydrogen atoms were included with idealized parameters. Data from the DMEDA−LiTf crystals were collected at 103(2) K. The final R1 = 0.047 is based on 2074 "observed reflections" [$I > 2\sigma(I)$], and wR2 = 0.146 is based on all reflections (2506 unique reflections). The triflate ion was modeled using two components with 50% occupancy for each component due to the presence of some static disorder. For the DMEDA−NaTf crystal, the data were collected at 90(2) K. The final R1 = 0.063 is based on 1584 observed reflections [$I > 2\sigma(I)$], and wR2 = 0.182 is based on all reflections (2197 unique reflections). The structural details and unit cell parameters of both crystals are described in the following section.

Infrared data were collected using a Bruker IFS66V FT-IR spectrometer (KBr beam splitter) under vacuum (11 mbar) for the crystalline samples and under dry air purge for the liquid samples. The data were recorded over a range of 500−4000 cm^{-1} at a spectral resolution of 1 cm^{-1}. The DMEDA−salt solutions were placed between zinc selenide windows in a sealed sample holder, and the crystalline samples were ground with potassium bromide and pressed into thin pellets. The Raman samples were sealed in a thin NMR tube under argon atmosphere. The data were recorded with a Jobin Yvon T64000 spectrometer. The 532 nm line of an Nd:YAG laser was used for excitation with a power of 200 mW measured at the laser head.

DSC thermograms were collected using a Mettler DSC 820 calorimeter under a dry nitrogen flow of 87 mL/min at heating and cooling rates of 5 °C/min. An 8−15 mg portion of crystalline material was sealed in 40 μL aluminum pans under argon atmosphere. The thermograms were analyzed using STAR^e v.6.10 software from Mettler Toledo.

TABLE 1: Structural Data for Crystalline Phases of DMEDA−LiTf and DMEDA−NaTf

	DMEDA−LiTf	DMEDA−NaTf
crystal system	monoclinic	monoclinic
space group	*P*2(1)/*c*	*P*2(1)/*c*
temperature (K)	103(2)	90(2)
a (Å)	6.5375(15)	11.477(12)
b (Å)	18.518(4)	9.717(10)
c (Å)	9.440(2)	11.283(12)
β(°)	93.479(3)	117.01(2)
volume (Å^3)	1140.7(5)	1121(2)
Z	4	4
density (Mg/m^3)	1.422	1.542
R1	0.0387	0.0634
crystal size (mm^3)	0.58 × 0.34 × 0.02	0.46 × 0.40 × 0.16

3. Results and Discussion

3.1. Crystalline Phases of *N,N*-DMEDA−LiTf and *N,N*-DMEDA−NaTf. The *N,N*-DMEDA−LiTf crystals form a monoclinic unit cell in the *P*2(1)/*c* space group, with four (DMEDA−LiTf) asymmetric units in the cell. A summary of the structural data is shown in Table 1.

The packing forms a polymeric one-dimensional network along the crystallographic *c* axis, as shown in Figure 1.

In this network, lithium coordinates both nitrogen atoms from a single DMEDA molecule and two oxygen atoms from different triflate anions (Figure 2).

The polymeric chain is basically composed of alternate triflate ions and DMEDA molecules, both coordinated by lithium ions. The different polymeric chains are held together by hydrogen-bonding interactions between the hydrogen atoms of the primary amine group of DMEDA and one triflate oxygen from an adjacent chain. The crystal structure shows some static disorder, which is accommodated by splitting the triflate group into two distinct positions of 52.5% and 47.7% occupancy for the unprimed and primed atoms, respectively. Only one position of the triflate ion is shown in the figures for purposes of clarity.

The *N,N*-DMEDA−NaTf crystal also forms a monoclinic unit cell in the *P*2(1)/*c* space group, with $Z = 4$ (DMEDA−NaTf) asymmetric units in the cell. Crystal data are also presented in Table 1. The packing diagram (Figure 3) shows the formation of a two-dimensional network parallel to the *bc* crystallographic plane.

A detailed picture of the coordination in Figure 4 shows that each sodium ion is bonded to two nitrogen atoms from one DMEDA molecule, and three oxygen atoms from different triflate anions. One of the primary amine hydrogen atoms forms a hydrogen bond with a triflate oxygen atom, while the other hydrogen atom forms a hydrogen bond with a fluorine atom of a different triflate anion (Table 2). The structure forms dimers in which one sodium ion coordinates to O1A and O2AA from two different triflate anions and the other sodium coordinates to O2A and O1AA of the same two triflate ions. The third oxygen atom of the two triflate ions—O3A and O3AA—coordinate to a sodium ion and extend the dimers into a network (Figure 4).

3.1.1. Comparison of the Crystal Structures. In each DMEDA−salt complex, the hydrogen atoms of the NH_2 group are hydrogen bonded (Table 2). In the DMEDA−LiTf crystal, each of the two hydrogen atoms is hydrogen bonded to an oxygen atom from a different triflate group, whereas, in the DMEDA−NaTf crystal, one hydrogen bond takes place with a triflate

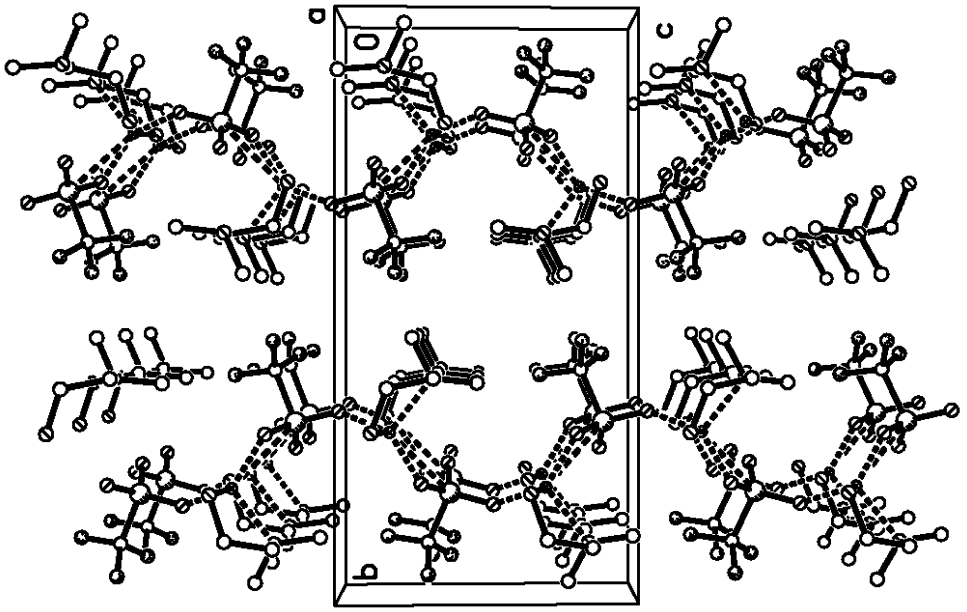

Figure 1. Packing diagram of the DMEDA−LiTf crystal projected down the crystallographic *a* axis. The crystal forms a polymeric one-dimensional network along the crystallographic *c* axis.

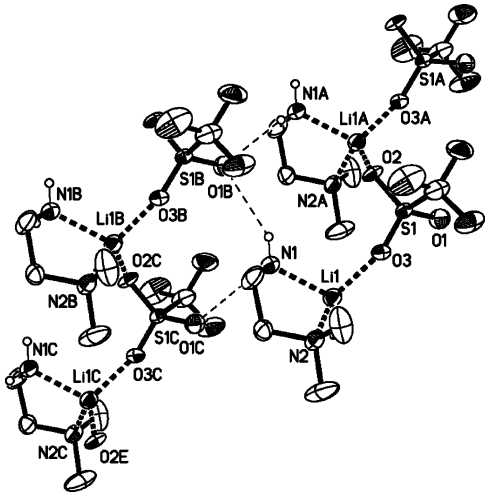

Figure 2. Crystal structure of DMEDA−LiTf showing the 4-fold coordination of lithium and the hydrogen-bonding environment of the primary amine groups.

oxygen, while the other hydrogen atom forms a hydrogen bond to a fluorine atom from a different triflate group. In both structures, the relatively large N−H···O and N−H···F distances, along with N−H−O and N−H−F angles that are significantly less than 180°, suggest that DMEDA forms weak hydrogen bonds with LiTf and NaTf. Moreover, in both crystal structures, it is important to note that there are no hydrogen-bonding interactions between the amine groups of DMEDA molecules. Structural details of the hydrogen bonds are summarized in Table 2.

The overall conformation of the DMEDA oligomers can be described by the torsional angles of the N−C−C−N and C−N−C−C bond sequences, where gauche (abbreviated g) is 60 ± 60°, trans (abbreviated t) is 180 ± 60°, and gauche minus (abbreviated $\bar{g}$) is 300 ± 60°. Particular attention is directed to the N−C−C−N angle, as it is directly affected by the coordination of the cation to the nitrogen atoms. In DMEDA−LiTf crystal, the N−C−C−N dihedral angle of the DMEDA molecule is gauche (59.0°), which results in *x*g conformations where *x* is the C−N−C−C dihedral angle and is either trans or gauche. In DMEDA−NaTf crystal, the N−C−C−N dihedral

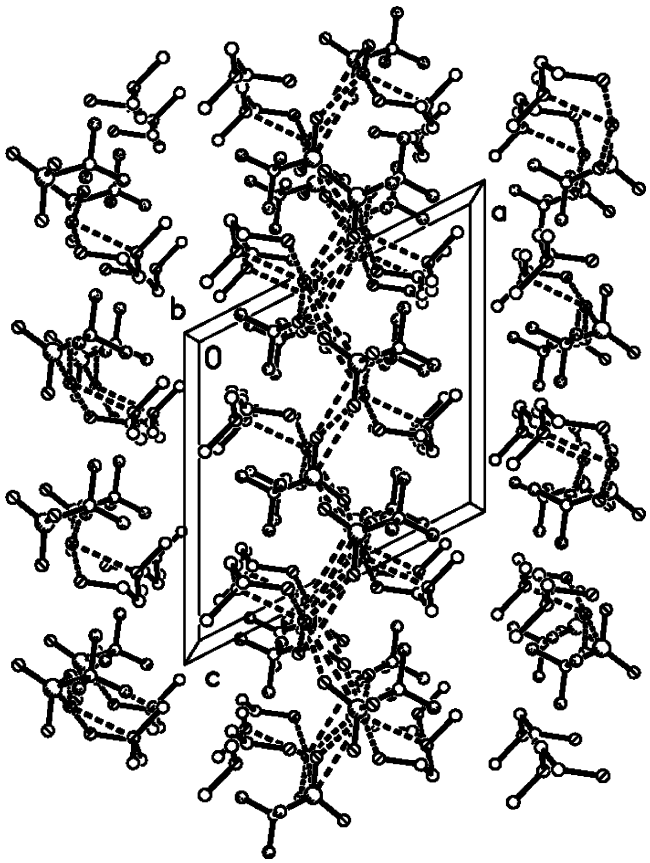

Figure 3. Packing diagram of the DMEDA−NaTf crystal projected down the crystallographic *b* axis. The crystal forms a polymeric two-dimensional structure in the *bc* crystallographic plane.

angle is gauche minus (−66.1°), which leads to *x*$\bar{g}$ conformations (*x* = t or $\bar{g}$) (Table 3). In Table 3, the last two rows for each crystal entry result from the two methyl groups terminating the nitrogen atoms. The DMEDA conformation in both crystals is similar to that previously observed in *N,N′*-DMEDA−NaTf crystal (t$\bar{g}$t and tgt).[19]

The cation−heteroatom bond distances are summarized in Table 4. In the DMEDA−LiTf crystal, the static disorder does

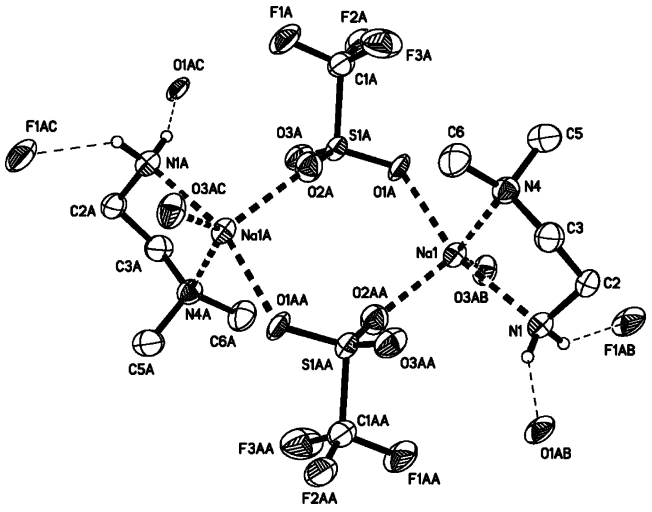

Figure 4. Crystal structure of DMEDA−NaTf showing the 5-fold coordination of sodium and the hydrogen-bonding environment of the primary amine groups. This picture highlights the formation of dimers.

not affect the lithium−oxygen coordination bond distance, as they are very similar for each position. The Li−N coordination bond distance is around 2.1 Å, while the Li−O bond length lies between 1.85 and 1.97 Å. In the sodium compound, the Na−N (∼2.5 Å) and Na−O (∼2.3 Å) bond lengths are much larger than the corresponding distances in the lithium compound. The difference between the lithium and sodium ionic radii is 0.29 Å,[20] which is smaller than the difference between the Li−N and Na−N bonds or the difference between the Li−O and Na−O bonds. This suggests that the lithium ion coordinates the nitrogen atom more strongly than does the sodium cation, which is consistent with the higher charge density of lithium. Furthermore, the N−Li−N angle is about 14.6° larger than the N−Na−N angle (Table 4). Considering that the N−C−C−N torsional angles are similar in the two compounds (Table 3), the 14.6° difference in the N−X^+−N angles (X^+ = Li^+, Na^+) is consistent with the differences in the cation−nitrogen coordination bond distances. Other nitrogen compounds such as *N*,*N*,*N*′,*N*′-tetramethylethylenediamine and hexamethyltriethylenetetramine also form complexes with lithium triflate and sodium triflate. The coordination bond distances and the N−X^+−N angles (X^+ = Li^+ or Na^+) in those complexes compare very well with those found in the DMEDA−LiTf and DMEDA−NaTf compounds.[21−23]

The *N*,*N*-DMEDA molecule contains two methyl groups attached to one of the nitrogen atoms and two hydrogen atoms on the other nitrogen atom. The difference in the steric accessibility of the two nitrogen atoms of the DMEDA molecule seems to have a small effect on the coordination of the cation. The Li−primary nitrogen bond length is 0.06 Å shorter than the Li−tertiary nitrogen bond length in the DMEDA−LiTf crystal. Similarly, the Na−primary nitrogen bond length in the DMEDA−NaTf crystal is 0.04 Å shorter than the Na−tertiary nitrogen bond distance (Table 4).

N,*N*-DMEDA also forms a crystalline phase with sodium tetraphenylborate ($NaBPh_4$).[24] In this compound, each sodium ion is coordinated to six nitrogen atoms from three DMEDA molecules, corresponding to a nitrogen-to-sodium ratio of 6:1. The BPh_4 anion does not participate in the coordination with the sodium cation, as it is bulky and charge protected. The sodium coordination geometry can be described as a very distorted octahedron. Again, the greater steric hindrance in the tertiary part of the DMEDA molecule does not seem to significantly affect its coordination with the cation, although larger differences between the tertiary and primary part of the molecule can be noted. The nitrogen−sodium bond distances lie around 2.45 and 2.51 Å for the primary amine nitrogen atoms and 2.61−2.67 Å for the tertiary nitrogen atoms, which represents a 0.1−0.2 Å difference. The disparity between DMEDA−NaTf and $(DMEDA)_3$−$NaBPh_4$ complexes can be explained by the packing requirement of the compounds: the DMEDA−NaTf complex forms a two-dimensional network in which one sodium coordinates to one DMEDA molecule and three oxygen atoms from different triflate anions; in the $(DMEDA)_3$−$NaBPh_4$ complex, three DMEDA molecules are clustered around one sodium cation, and the steric hindrance becomes an important factor.

3.1.2. Thermal Analysis. DSC was used to study the melting and recrystallization processes in the crystals. In the DSC thermogram of the DMEDA−NaTf crystal, a sharp endotherm occurs with an onset at 41 °C (midpoint = 47 °C), and the onset of recrystallization occurs at 21 °C (midpoint = 17 °C). In a subsequent thermal cycle, the onset temperatures of melting and recrystallization decrease to 38 °C (midpoint = 43 °C) and 17 °C (midpoint = 15 °C), respectively, which suggests some degree of thermal hysteresis. Upon further cycling, the melting peak becomes smaller and broader, probably caused by a loss of crystallinity of the sample.

The DSC thermograms of the DMEDA−LiTf crystal are not as straightforward. First, the DMEDA−LiTf crystal was cycled between 0 and 60 °C. During the first heating period (25−60 °C), a sharp endothermic peak occurs with an onset at 48 °C (midpoint = 54 °C) due to the melting of the crystalline compound. In the cooling phase, two exothermic transitions are observed with onsets at 8 °C (midpoint = 6 °C) and ∼19 °C (midpoint = 16 °C). In a second thermal cycle, two endothermic peaks are observed in the heating portion, with onsets at 8 °C (midpoint = 13 °C) and 45 °C (midpoint = 49 °C), and, upon cooling, the onsets are observed at 8 °C (midpoint = 5 °C) and 18 °C (midpoint = 15 °C), respectively. When more thermal cycles are performed (between 0 and 60 °C), the onsets of these thermal transitions keep slowly decreasing. This may indicate some degree of thermal hysteresis. When the DMEDA−LiTf crystal is cycled between 0 and 150 °C, the first endotherm occurs with an onset at 48 °C (midpoint = 54 °C) (first cycle between 25 and 150 °C). In the following cooling and reheating periods, the onsets of the thermal transitions described above behave in a similar manner, but a third endotherm starts to appears at higher temperatures. This third transition peak does not remain at a constant temperature. In the second heating cycle, the endotherm is small and occurs with an onset around 57 °C (midpoint = 80 °C) (the onset of the exotherm is observed at 61 °C (midpoint = 55 °C) in the following cooling period), and, in the fourth cycle, it is at 92 °C (midpoint = 104 °C) (the onset of the exotherm is observed at 110 °C (midpoint = 105 °C) in the following cooling period). The appearance of the third endothermic peak might indicate the formation of a new crystalline phase at higher temperatures or the incongruent melting of the DMEDA−LiTf crystal. However, these experiments have not been taken further because they would be outside the scope of this paper.

3.2. Vibrational Spectroscopy. *3.2.1. N−H Stretching Region of DMEDA and DMEDA in CCl_4.* The NH stretching modes of a primary amine consist of the antisymmetric NH_2 stretch, $\nu_{as}(NH_2)$, and the symmetric NH_2 stretch, $\nu_s(NH_2)$. Although these labels are strictly accurate only for an isolated NH_2 group, they will be used throughout this paper to describe the vibrations of the primary amine group undergoing a variety

TABLE 2: Hydrogen Bond Parameters for the DMEDA−LiTf Crystal and the DMEDA−NaTf Crystal[a]

	N−H···A[b]	*d* (N−H)	*d* (H···A)	*d* (N···A)	angle (NHA)
DMEDA−LiTf	N(1)−H(1D)···O(1) #3	0.84	2.28	3.013(5)	147(2)
	N(1)−H(1D)···O(1′) #3	0.84	2.28	3.083(6)	162(2)
	N(1)−H(1E)···O(1) #4	0.82	2.54	3.284(5)	150(2)
	N(1)−H(1E)···O(1′) #4	0.82	2.41	3.185(6)	157(2)
DMEDA−NaTf	N(1)−H(1A)···O(1A)	0.89	2.43	3.242(6)	153(5)
	N(1)−H(1B)···F(1A)	0.92	2.34	3.131(6)	144(4)

[a] All bond distances are in angstroms (Å). [b] Symmetry transformation used to generate equivalent atoms: (#3) $x + 1, -y + 3/2, z + 1/2$; (#4) $x + 1, y, z$.

TABLE 3: Torsional Angles of DMEDA−LiTf and DMEDA−NaTf Crystals and the Corresponding Conformations

bond sequence	torsional angle (°)	conformation
	DMEDA−LiTf	
N1−C3−C4−N2	59.0(3)	g
C1−N2−C4−C3	−162.3(2)	t
C2−N2−C4−C3	76.8(2)	g
	DMEDA−NaTf	
N1−C2−C3−N4	−66.1(6)	$g\bar{g}$
C5−N4−C3−C2	−75.2(5)	$g\bar{g}$
C6−N4−C3−C2	163.5(4)	t

TABLE 4: Selected Bond Lengths (Å) and Angles (°) for the DMEDA−LiTf and DMEDA−NaTf Crystals

	bond distance X−N	bond distance X−O	angle (NXN)
X = Li	2.100(4) tertiary	1.932(7)	88.38(13)
	2.039(3) primary	1.942(9)	
		1.968(7)	
		1.848(8)	
X = Na	2.507(5) tertiary	2.293(4)	73.80(15)
	2.466(5) primary	2.314(4)	
		2.370(4)	

of perturbations. The frequencies and intensities of $\nu_{as}(NH_2)$ and $\nu_s(NH_2)$ in the IR and Raman spectra provide an excellent spectroscopic tool to study hydrogen bonding and, upon addition of salt, ion−molecule interactions. Electronic redistribution accompanying these interactions changes the intensities and shifts the frequencies of the NH stretching vibrations, providing a useful probe of the underlying interactions.[25,26] The characteristic N−H stretching frequency decrease that signals hydrogen bonding is well-known; however, band intensity changes can be equally important. For example, in an isolated NH_2 group, $\nu_s(NH_2)$ exhibits strong Raman scattering and weak infrared absorption, whereas the converse is true for $\nu_{as}(NH_2)$. If only one hydrogen atom of a primary amine group forms a hydrogen bond, the intensity and the frequency of the symmetric stretch will be significantly affected as the symmetric character of the mode is altered. However, the antisymmetric stretch will not be as sensitive to such perturbation because it is already asymmetric in nature.

Infrared spectra of the NH stretching region are plotted in Figure 5 for dilute solutions of hexylamine, benzylamine, and DMEDA dissolved in carbon tetrachloride (CCl_4). Each solution is prepared at a molar ratio of 30:1 CCl_4:NH_2. In these dilute solutions, the intermolecular hydrogen-bonding interactions are essentially eliminated.[27,28] The $\nu_s(NH_2)$ band occurs at 3326, 3327, and 3320 cm^{-1} in solutions of hexylamine, benzylamine, and DMEDA, respectively, while the $\nu_{as}(NH_2)$ mode is observed at 3392, 3396, and 3394 cm^{-1}, respectively. There is also a noticeable low-frequency shoulder on the DMEDA $\nu_{as}(NH_2)$ band. A comparison of the $\nu_s(NH_2)$ bands shows that the vibrational potential energy environments of hexylamine and benzylamine are identical within experimental error. However, the lower frequency of the DMEDA $\nu_s(NH_2)$ band (∼6−7 cm^{-1}) suggests that some fraction of the molecules experiences a weak

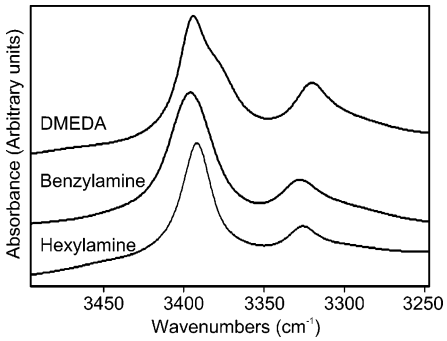

Figure 5. Infrared spectra of the N−H stretching region for solutions of hexylamine, benzylamine, and DMEDA dissolved in carbon tetrachloride at a molar ratio of 30:1 CCl_4:NH_2.

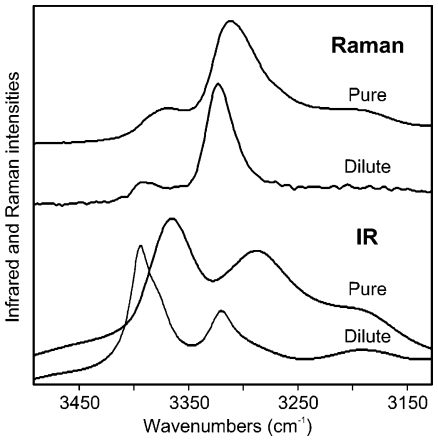

Figure 6. Raman (top) and infrared (bottom) spectra of the N−H stretching region for pure DMEDA and DMEDA dissolved in carbon tetrachloride at a molar ratio of 30:1 CCl_4:NH_2.

hydrogen-bonding interaction that does not occur in hexylamine and benzylamine. This is attributed to *intramolecular* hydrogen bonding between a primary amine hydrogen atom and the tertiary amine nitrogen atom. Support for this hypothesis is provided by the low-frequency shoulder on the DMEDA $\nu_{as}(NH_2)$ band. This feature also argues that some fraction of the DMEDA molecules are undergoing a hydrogen-bonding interaction not experienced by either benzylamine or hexylamine. Unpublished computational studies show that the conformation leading to intramolecular hydrogen bonding is energetically stable.[29]

Figure 6 compares the IR and Raman spectra of pure DMEDA and dilute solutions of DMEDA dissolved in CCl_4. The IR spectrum of pure DMEDA contains a strong $\nu_{as}(NH_2)$ band centered at 3366 cm^{-1} and a weaker, broader $\nu_s(NH_2)$ band at 3288 cm^{-1}. The less intense shoulder at roughly 3192 cm^{-1} is an overtone of the NH_2 deformation band at 1596 cm^{-1} and is also seen in the IR spectrum of the dilute DMEDA−CCl_4 solution. The extensive hydrogen-bonding interactions of pure DMEDA shift the "isolated" NH_2 stretching frequencies (relative to the values in the dilute CCl_4 solution) by $\Delta\nu_{as}(NH_2) = -28$

TABLE 5: N−H Stretching Frequencies (cm^{-1}) of Pure *N,N*-DMEDA and *N,N*-DMEDA Dissolved in CCl_4 at a Molar Ratio of 30:1 CCl_4:NH_2

		DMEDA	DMEDA in CCl_4
IR	$\nu_{as}(NH_2)$	3366	3394
	$\nu_s(NH_2)$	3288	3320
Raman	$\nu_{as}(NH_2)$	3370	3392
	$\nu_s(NH_2)$	3311	3323

cm^{-1} and $\Delta\nu_s(NH_2) = -32$ cm^{-1}. The frequency data are summarized in Table 5.

An interesting story emerges from the comparison of the two Raman spectra of Figure 6. In the dilute CCl_4 solution, the maximum of $\nu_s(NH_2)$ occurs at 3323 cm^{-1} in the Raman spectrum, which is intermediate between the IR frequency of $\nu_s(NH_2)$ in dilute solutions of hexylamine and benzylamine in CCl_4 and the dilute solution of DMEDA in CCl_4 shown in Figure 5. In the dilute solutions of hexylamine and benzylamine, there were no intermolecular or intramolecular hydrogen-bonding interactions. It appears that the Raman spectrum of DMEDA in the $\nu_s(NH_2)$ region selectively samples those DMEDA molecules that also experience minimal intermolecular or intramolecular hydrogen-bonding interactions. This selectivity results from the highly symmetric nature of those NH_2 vibrations. In the Raman spectrum of pure DMEDA, the $\nu_s(NH_2)$ band occurs at 3311 cm^{-1}, which is about 12 cm^{-1} lower than the corresponding band in the dilute CCl_4 solution. In a study of hexylamine, which contains only a single primary amine group and in which intramolecular hydrogen bonding is therefore impossible, the frequencies of the Raman bands of $\nu_s(NH_2)$ in pure hexylamine and in a dilute CCl_4 solution were quite close (3324 and 3328 cm^{-1}). Therefore, the larger frequency difference observed between pure and dilute CCl_4 solutions of DMEDA is attributed to the fraction of molecules undergoing intramolecular hydrogen-bonding interactions. These interactions may be present to a somewhat greater extent in the CCl_4 solution than in pure DMEDA because the intermolecular hydrogen-bonding interactions present in pure DMEDA would be expected to decrease the number of nitrogen sites available for intramolecular hydrogen-bonding interactions. In the IR and Raman spectra of the CCl_4 solutions, the frequencies of $\nu_s(NH_2)$ are almost coincident: 3320 cm^{-1} in the IR and 3323 cm^{-1} in the Raman. This is because the bands originate in the vibrations of the NH_2 groups in which intermolecular hydrogen bonding does not occur. The same near coincidence is also observed for the $\nu_{as}(NH_2)$ band: 3394 cm^{-1} in IR and 3392 cm^{-1} in Raman. In the IR spectrum of the dilute solution, $\nu_{as}(NH_2)$ exhibits a shoulder on the low-frequency side, and $\nu_s(NH_2)$ has a long tail that extends beneath the pure DMEDA $\nu_s(NH_2)$ IR band. Both features originate in the population distribution of hydrogen-bonded DMEDA molecules.

Finally, in pure DMEDA, the frequency differences between the IR and Raman band maxima are 4 cm^{-1} for $\nu_{as}(NH_2)$ and 23 cm^{-1} for $\nu_s(NH_2)$. These differences confirm that the frequency of the $\nu_s(NH_2)$ mode is more sensitive to hydrogen-bonding interactions. The sensitivity arises because, in the pure liquid, the Raman spectrum selectively picks out those molecules whose vibrations are the most symmetric, that is, undergoing the least amount of hydrogen-bonding interactions.

3.2.2. N−H Stretching Region of DMEDA−LiTf and DMEDA−NaTf Solutions. The effect of adding salt to DMEDA is illustrated in Figure 7, which shows the Raman spectra of DMEDA−LiTf in the NH stretching region.

The broad $\nu_s(NH_2)$ band at 3311 cm^{-1} in pure DMEDA appears to shift to lower frequencies with increasing salt concentration, although this shift may result from an increase in scattering intensity on the low-frequency side, perhaps accompanied by an intensity decrease of the original maximum in the band envelope. At a 10:1 composition, the band maximum is at 3302 cm^{-1} in the LiTf solution. With further addition of salt, $\nu_s(NH_2)$ then shifts to higher frequencies until, at a 3:1 composition, the band maximum is at 3314 cm^{-1}. This trend continues on into the crystalline phase, where there is a single $\nu_s(NH_2)$ band at 3316 cm^{-1}. These frequency data are plotted in Figure 8, along with the corresponding data for the NaTf solutions (spectra not shown).

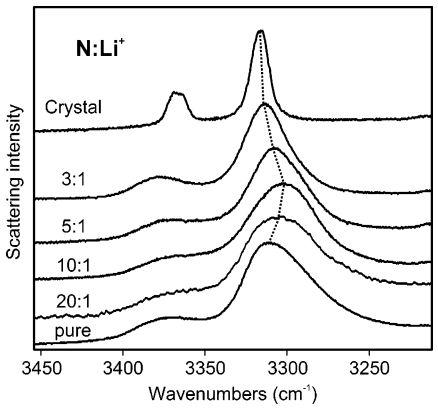

Figure 7. Raman spectra of DMEDA−LiTf crystal, DMEDA−LiTf solutions with various $N:Li^+$ ratios, and pure DMEDA in the N−H stretching region.

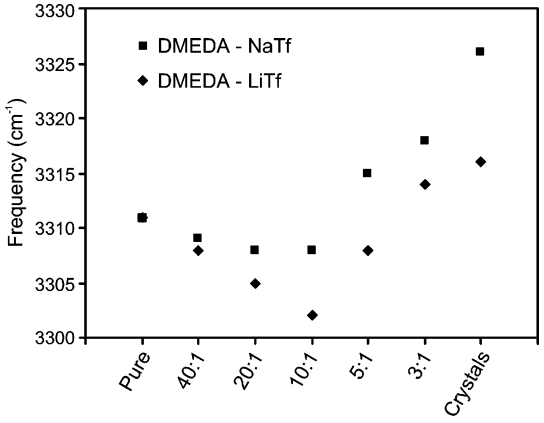

Figure 8. Summary of the NH_2 symmetric stretch frequencies of DMEDA−LiTf and DMEDA−NaTf solutions at various $N:M^+$ ratios, and the respective crystals.

In pure DMEDA, the Raman spectrum of $\nu_s(NH_2)$ selectively samples those DMEDA molecules that undergo the weakest hydrogen-bonding interactions.[30] The frequency shift results from a combination of two opposing factors. The cation coordination effect shifts the bands to lower frequencies because the lone pair of the nitrogen atom is involved in the solvation of the cations, causing a weakening of the N−H bond by decreasing its electron density. However, the intermolecular or intramolecular hydrogen bonds in DMEDA are replaced by weaker hydrogen bonds to the triflate oxygen atoms, causing a shift to higher frequencies. Therefore, the resulting frequency of an N−H stretching band is dependent on the relative contribution of each factor. Noting that, in the crystals, there are only N−H···O hydrogen bonds present, it is clear from comparing the frequencies in pure DMEDA with those in the DMEDA−LiTf crystalline phase that the N−H···O hydrogen bond is weaker than the N−H···N hydrogen bond. For example, $\nu_s(NH_2)$ in the Raman spectrum of the crystal is at 3316 cm^{-1},

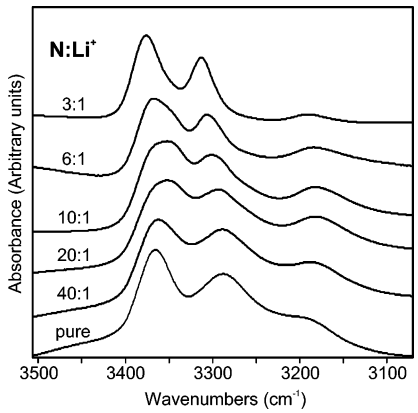

Figure 9. Infrared spectra of DMEDA−LiTf solutions with various $N:Li^+$ ratios, and pure DMEDA in the N−H stretching region.

which is 5 wavenumbers higher than the value in pure DMEDA. This is despite the fact that the cation coordination effect in the crystal will shift the frequency to lower values.

The initial shift to lower frequencies at low salt concentrations occurs because the cation coordinates those DMEDA molecules that are essentially "free" and therefore more accessible for coordinative interaction, and the cation coordination effect is dominant. Apparently, in the more dilute solutions, the weaker N−H···O hydrogen bonds do not tend to form. However, as additional salt is added, the population of more strongly N−H···N hydrogen-bonded DMEDA molecules is replaced by DMEDA molecules that are either more weakly hydrogen bonded to triflate oxygen atoms or perhaps not hydrogen bonded at all. This effect more than compensates for the decrease due to the cation coordination effect, and the frequency of the NH stretching bands increases.

Qualitatively, the same behavior seen in the DMEDA-LiTf solutions occurs in the DMEDA−NaTf solutions (see Figure 8), that is, the $\nu_s(NH_2)$ frequency first decreases and then increases with increasing salt composition. Although the minimum occurs at the same 10:1 composition, the frequency shift from the pure liquid is not as large as it is in the LiTf solutions. Moreover, the frequency of $\nu_s(NH_2)$ is 10 wavenumbers higher (3326 cm^{-1}) in the DMEDA−NaTf crystal than it is in the DMEDA−LiTf crystal (3316 cm^{-1}). This comparison argues that the cation coordination effect is weaker in the DMEDA−NaTf crystal than it is in the DMEDA−LiTf crystal.

Figure 9 shows the IR spectra of DMEDA−LiTf solutions in the N−H stretching region. With increasing salt concentration, the frequency of $\nu_{as}(NH_2)$ behaves similarly to shifts observed in the Raman spectrum of $\nu_s(NH_2)$, illustrated in Figure 7. The band at 3366 cm^{-1} in pure DMEDA shifts to lower frequencies until a minimum of about 3352 cm^{-1} is observed in the 10:1 composition. With further addition of salt, the band then shifts to higher frequencies. As in the case of the Raman spectra of $\nu_s(NH_2)$, the "shift" of $\nu_{as}(NH_2)$ appears to be a poorly resolved band that grows on the low-frequency side of $\nu_{as}(NH_2)$, until, at the 10:1 composition, the band appears as a broad feature with poorly defined structure. In the 6:1 composition, the lower frequency feature is now a shoulder at roughly 3351 cm^{-1} on the side of the dominant 3367 cm^{-1} band. In the 3:1 sample, there is only a well-defined band at 3376 cm^{-1}. The initial "shift" to lower frequencies at lower salt concentrations is again due to the cation coordination effect. At higher salt concentrations, the breaking of N−H···N hydrogen bonds results in a shift to higher frequencies.

In contrast to the $\nu_{as}(NH_2)$ behavior in the IR spectrum, $\nu_s(NH_2)$ at 3288 cm^{-1} in pure DMEDA continuously shifts to higher frequencies with increasing LiTf concentration, finally reaching 3313 cm^{-1} at the 3:1 composition. The failure to observe any initial decrease in frequency due to the cation coordination effect is attributed to the greater sensitivity of the $\nu_s(NH_2)$ mode to hydrogen bonding. A study of tetrabutylammonium triflate dissolved in DMEDA supports this point (spectral data not shown). The bulky nature of the tetrabutylammonium cation prevents any coordination with the DMEDA host; consequently, these measurements isolate the effect of hydrogen-bond replacement. In a DMEDA−tetrabutylammonium triflate solution at a 3:1 composition, the $\nu_{as}(NH_2)$ and $\nu_s(NH_2)$ bands occur at 3371 and 3307 cm^{-1}, respectively. Relative to pure DMEDA, these are shifts of +5 and +19 cm^{-1}, which shows that $\nu_s(NH_2)$ is considerably more sensitive to hydrogen-bonding interactions. Consequently, in the DMEDA−LiTf solutions, the replacement of N−H···N hydrogen bonds by weaker N−H···O hydrogen bonds more than compensates for the cation coordination effect, and a continuous higher frequency shift of $\nu_s(NH_2)$ with increasing salt concentration is observed.

Patterns of spectral behavior found in the IR data of DMEDA−NaTf solutions are similar to those of DMEDA−LiTf solutions, although the presence of the lower frequency feature on the side of $\nu_{as}(NH_2)$ is barely visible. The shift of $\nu_s(NH_2)$ from pure DMEDA to a 3:1 composition is +29 cm^{-1}, which is greater than the +25 cm^{-1} shift in the corresponding LiTf solution. An analogous pattern is found for $\nu_{as}(NH_2)$: the shift is +15 cm^{-1} in the 3:1 composition of DMEDA−NaTf and only +10 cm^{-1} in the corresponding DMEDA−LiTf complex.

It is noteworthy that, at the 3:1 composition, the $\nu_s(NH_2)$ stretching frequencies of the IR and Raman bands are coincident (within experimental error) in both the LiTf and NaTf solutions, with the frequencies of the NaTf solutions somewhat higher; the same is true of $\nu_{as}(NH_2)$. At this very high salt concentration, the hydrogen-bonding environment of the molecules is quite similar, as is their coordination with the cations. Therefore, the Raman and IR selection rules cannot distinguish molecules within the general population, and the bands are coincident.

3.2.3. N−H Stretching Region of DMEDA−LiTf and DMEDA−NaTf Crystals. In the crystalline phase, the $\nu_{as}(NH_2)$ vibrations of DMEDA−LiTf and the $\nu_s(NH_2)$ vibrations of DMEDA−NaTf are split into several components. The IR and Raman spectra of the two crystals are shown in Figure 10, and the data are summarized in Table 6.

This pattern results from the intermolecular coupling of vibrating NH_2 groups in the primitive unit cell; the number of normal modes and their symmetry classification can be calculated using standard group theory methods.[31] Because both crystals belong to the same space group, they have the same unit cell group. Therefore, a similar vibrational pattern is expected for both crystals. The vibrational modes originating in each kind of NH stretch and their classification according to the irreducible representations of the C_{2h} unit cell group (factor group) are

$$\Gamma(\nu_s(NH_2)) = \Gamma(\nu_{as}(NH_2)) = A_g + B_g + A_u + B_u \quad (1)$$

Two infrared active modes and two Raman active modes are predicted for each of the $\nu_s(NH_2)$ and $\nu_{as}(NH_2)$ vibrations in the crystal. In the IR spectrum of the DMEDA−NaTf crystal, $\nu_s(NH_2)$ has two distinct peaks at 3327 and 3343 cm^{-1}, and $\nu_{as}(NH_2)$ has one main band at 3399 cm^{-1} with a shoulder around 3406 cm^{-1}. In the DMEDA−LiTf crystal, $\nu_s(NH_2)$ occurs at 3316 cm^{-1} with two distinct shoulders on each side, while $\nu_{as}(NH_2)$ clearly splits into two major components at 3358

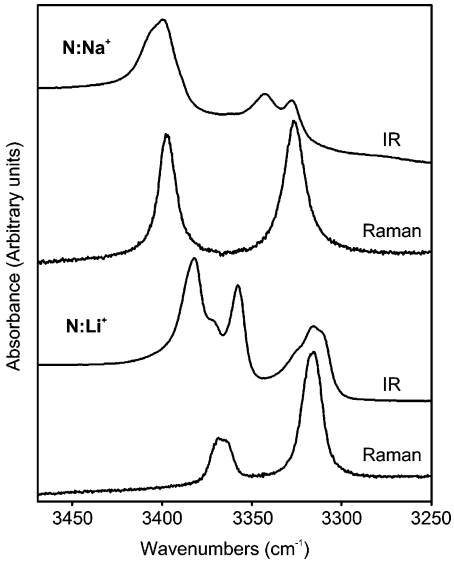

Figure 10. Raman and infrared spectra of DMEDA−NaTf crystal (top) and DMEDA−LiTf crystal (bottom) in the N−H stretching region.

TABLE 6: N−H Stretching Frequencies (cm^{-1}) of DMEDA−LiTf and DMEDA−NaTf Crystals

		$\nu_{as}(NH_2)$	$\nu_s(NH_2)$
DMEDA−LiTf	Raman	3366	3316
	IR	3382	3316
		3371 (sh)	
		3358	
DMEDA−NaTf	Raman	3398	3326
	IR	3406 (sh)	3343
		3399	3327

and 3382 cm^{-1} with a shoulder at roughly 3371 cm^{-1}. Because the sample is in the form of a microcrystalline powder when the spectra are measured, these minor "extra" features may originate in orientational effects. However, it is curious that these occur in the DMEDA−LiTf crystal, but not in the DMEDA−NaTf crystal.

The importance of the cation coordination effect is apparent when comparing the spectra of the 3:1 solutions with those of the crystals. In the LiTf system, the $\nu_s(NH_2)$ and $\nu_{as}(NH_2)$ bands occur at about the same frequencies in both the 3:1 solution ($\nu_s(NH_2) = 3314$ cm^{-1}, Raman) and in the crystal ($\nu_s(NH_2) = 3316$ cm^{-1}, Raman), whereas, in the DMEDA−NaTf system, the same comparison shows a striking shift to higher frequencies in the crystal ($\Delta\nu_s(NH_2) = +8$ cm^{-1}). In the 3:1 solutions, there is still a significant amount of N−H···N hydrogen-bonding interactions that are not broken until the crystals are formed. The crystal structures of both compounds clearly show that the N−H···N hydrogen bonds present in the solution phase have been replaced by weaker hydrogen bonds with the triflate oxygen atoms in the DMEDA−LiTf compound; in the DMEDA−NaTf compound, there is also a weak hydrogen bond with a fluorine atom (Table 2). Consequently, the difference between the two systems is most easily explained by the stronger coordination effect of the lithium ion. The coordination effect of sodium is not strong enough to compensate for breaking the hydrogen bonds that occur in the solution phase; consequently, there is a marked shift to higher frequencies upon the formation of the crystalline phase. On the other hand, in the DMEDA−LiTf crystal, the relatively stronger lithium ion coordination effect lowers the frequency, almost offsetting the shift to higher frequency that accompanies the replacement of relatively stronger hydrogen bonds in solution by weaker hydrogen bonds in the crystal.

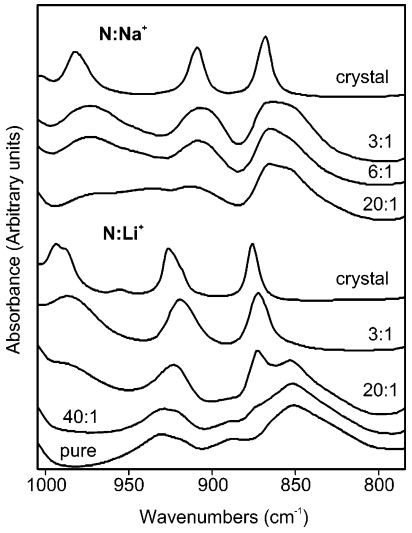

Figure 11. Infrared spectra of DMEDA−NaTf solutions (top) and DMEDA−LiTf solutions (bottom) with various $N:M^+$ ratios and the corresponding crystals in the conformation region.

The symmetry-based vibrational analysis (eq 1) predicts two Raman active modes for each of the two NH stretching modes. In the Raman spectrum of the DMEDA−LiTf crystalline compound, $\nu_s(NH_2)$ has a small sharp peak centered at 3316 cm^{-1}, a frequency corresponding to one of the IR bands, whereas $\nu_{as}(NH_2)$ occurs around 3366 cm^{-1} with a much smaller scattering intensity and does not have a counterpart in the IR spectrum. The band shape of $\nu_{as}(NH_2)$ suggests two underlying components, accounted for by the predicted factor group multiplet of eq 1. In the DMEDA−NaTf crystal, the NH stretching region of the Raman spectrum exhibits two relatively sharp peaks of similar intensity: $\nu_s(NH_2)$ at 3326 cm^{-1} and $\nu_{as}(NH_2)$ at 3398 cm^{-1}. These frequencies are coincident within experimental error with two of the IR bands.

The relative Raman intensities of $\nu_{as}(NH_2)$ and $\nu_s(NH_2)$ in the two compounds can be explained in terms of their crystal structures. In the DMEDA−LiTf crystal (Figure 2), each hydrogen atom of the NH_2 groups is weakly hydrogen bonded to an oxygen atom of a triflate ion, with the hydrogen-bonding environment of each amine hydrogen atom roughly equivalent. Therefore, the $\nu_{as}(NH_2)$ and $\nu_s(NH_2)$ modes preserve their approximately antisymmetric and symmetric character, respectively, as reflected in the IR and Raman intensities of each mode. In contrast, in the DMEDA−NaTf crystal (Figure 4), the hydrogen atoms of the NH_2 group form hydrogen bonds to an oxygen atom and to a fluorine atom. The significantly different potential energy environment of the two hydrogen atoms causes the $\nu_{as}(NH_2)$ and $\nu_s(NH_2)$ modes to lose their symmetric and antisymmetric character, as it is reflected in the intensities in the Raman spectrum. Interestingly, the relative IR intensities of the two modes appear to be insensitive to subtle differences in the potential energy environment of the two crystals.

3.2.4. Conformation of DMEDA. Figure 11 shows the IR spectra from 800 to 1000 cm^{-1} of DMEDA, solutions of DMEDA−LiTf and DMEDA−NaTf at various compositions, and the corresponding DMEDA−salt crystals. Frequencies and intensities of bands in this spectral region are particularly sensitive to the coordinative interactions between the DMEDA nitrogen atoms and the cations. In DMEDA, the bands in this region are mainly comprised of a mixture of CH_2 rocking, C−N stretching, and NH_2 wagging motions, plus a small contribution from C−C stretching. With the addition of LiTf or NaTf, the CH_2 rocking and NH_2 wagging motions provide the primary

contribution to the normal modes. These assignments are based on gas-phase quantum chemical calculations of pure DMEDA, DMEDA−LiTf, and DMEDA−NaTf systems.[29] In the IR spectrum, DMEDA has three bands of medium intensity at 851, 887, and 930 cm^{-1}, with a weak band at 918 cm^{-1}. As LiTf is initially added to DMEDA, a small, sharp band appears on the high-frequency side of the 851 cm^{-1} band at roughly 873 cm^{-1}. Upon further addition of salt, the intensity of this band increases, but the frequency does not shift until crystal formation, where the band occurs at 876 cm^{-1}. With the addition of NaTf to DMEDA, similar behavior is observed. A new band appears at about 865 cm^{-1}, on the high-frequency side of the 851 cm^{-1} DMEDA band. The new band increases in intensity with increasing salt concentration until the original 851 cm^{-1} band is a weak, high-frequency shoulder in the 6:1 composition. In the 3:1 composition, only one very broad band is observed. This band becomes much sharper in the crystal and shifts to 868 cm^{-1}.

Two other DMEDA bands in this region are markedly changed by the addition of salt. The band at 930 cm^{-1} appears to initially broaden as LiTf is added, although this may be due to coalescence with the low-frequency feature at 918 cm^{-1} (clearly seen in the spectrum of pure DMEDA). The frequency of the band decreases with LiTf concentration to 919 cm^{-1} in the 3:1 sample, and shifts to 926 cm^{-1} in the crystalline phase, with two distinct shoulders on the low-frequency side. At the same time, a weak, broad band appears at roughly 989 cm^{-1} (20:1 composition) and grows in intensity until it is a very distinct feature at 987 cm^{-1} in the 3:1 sample. This band then appears as two bands at 994 and 988 cm^{-1} in the crystal. The behavior with the addition of NaTf appears to be somewhat different. The spectrum of the 20:1 sample suggests that the intensity of the DMEDA band at 930 cm^{-1} decreases and its frequency increases, appearing as a weak feature at 935 cm^{-1}. At the same time, the intensity of the 918 cm^{-1} band grows as the frequency decreases to 913 cm^{-1}. In the 3:1 sample, this band is centered roughly at 909 cm^{-1} and appears as a sharp band in the crystal at 907 cm^{-1}. In addition, a weak, broad band at 970 cm^{-1} is observed in the 20:1 spectrum and becomes a very broad feature centered roughly at 973 cm^{-1} in the 3:1 composition. The band then shifts to 982 cm^{-1} in the DMEDA−NaTf crystal.

The frequency shifts in this region are larger in the LiTf solutions than in the NaTf solutions, consistent with a stronger coordinative interaction of the lithium ion with DMEDA. Moreover, the bands that appear with the addition of salt are much narrower in the LiTf solutions than in the NaTf solutions at all comparable compositions. The smaller bandwidths in the LiTf solutions reflect a narrower distribution of DMEDA−Li^+ coordinative interactions, which presumably originate in the stronger DMEDA−Li^+ interactions. The crystallographic data show that the N−C−C−N angles in the DMEDA−LiTf and DMEDA−NaTf crystals are 59° and −66°, or g and $\bar{g}$, respectively. Although these dihedral angles differ by only 7°, this value probably reflects the difference in the strength of the cation−nitrogen atom coordination.

4. Conclusions

The comparison of the IR and Raman spectra of pure DMEDA and DMEDA dissolved in CCl_4 provides important information about the nature of the hydrogen-bonding interactions in DMEDA. In the infrared, the symmetric NH stretch was found to be more sensitive to the hydrogen-bonding environment of the primary amine group than the antisymmetric NH stretch. In the Raman spectrum, the $\nu_s(NH_2)$ band essentially samples the amine groups that are the least hydrogen bonded.

Upon addition of salt, there is a competition between hydrogen-bonding interactions in the DMEDA molecules and the coordination of the cation to the nitrogen atoms. At low salt concentrations (≤10:1), frequency shifts in the IR and Raman spectra of the LiTf system indicate the presence of both phenomena and show that the coordination of the Li cation is the predominant factor affecting the frequencies of the NH stretching bands. In the NaTf system, only the Raman spectra show this trend, as the coordination effect of sodium is weak and the shifts accompanying its effect are small. At higher salt concentrations, the breaking of intermolecular hydrogen bonding between DMEDA molecules controls the ν(NH) frequencies. This statement is confirmed by a comparison between the spectra of the crystals and the 3:1 solutions, where there is a significantly higher frequency shift in the DMEDA−NaTf crystal compared to the shift in the 3:1 solution. In the DMEDA−LiTf system, the NH stretching frequencies in the crystal and the 3:1 solution are similar due to the strong coordination effect of lithium. However, the frequencies are still much higher than those in pure DMEDA because of the extensive intermolecular hydrogen-bonding interactions in the pure solvent.

In the crystals, DMEDA molecules are hydrogen bonded to the oxygen atoms of the triflate anion in DMEDA−LiTf and to the triflate oxygen and the triflate fluorine atoms in DMEDA−NaTf. The presence of these hydrogen bonds does not seem to affect the frequency of the NH stretching modes to a significant extent; however, the bonding has an effect on the relative intensity of the symmetric and antisymmetric stretch in both the IR and Raman spectra. It is noteworthy that no hydrogen bonds occur between DMEDA molecules in the crystals.

References and Notes

(1) Bruce, P. G. *Faraday Discuss. Chem. Soc.* **1989**, *88*, 43.
(2) Papke, B. L.; Ratner, M. A.; Shriver, D. F. *J. Electrochem. Soc.* **1982**, *129*, 1434.
(3) Armand, M. B.; Chabagno, J. M.; Duclot, M. J. Polyethers as solid electrolytes. In *Fast Ion Transport in Solids*; Vashista, P., Mundy, J. M., Shenoy, G. K., Eds.; Elsevier: Amsterdam, 1979; p 131.
(4) Rocher, N. M.; Frech, R. *Macromolecules* **2005**, *38*, 10561.
(5) Frech, R.; Huang, W.; Dissanayake, M. A. K. L. *Mater. Res. Soc. Symp. Proc.* **1995**, *369*, 523.
(6) Schantz, S.; Sandahl, J.; Borjesson, L.; Torell, L. M.; Stevens, J. R. *Solid State Ionics* **1988**, *28−30*, 1047.
(7) Huang, W.; Frech, R.; Wheeler, R. A. *J. Phys. Chem.* **1994**, *98*, 100.
(8) Papke, B. L.; Ratner, M. A.; Shriver, D. F. *J. Phys. Chem. Solids* **1981**, *42*, 493.
(9) Ratner, M. A.; Nitzan, A. *Faraday Discuss. Chem. Soc.* **1989**, *88*, 19.
(10) Ratner, M. A.; Johansson, P.; Shriver, D. F. *MRS Bull.* **2000**, *25*, 31.
(11) Frech, R.; Huang, W. *Macromolecules* **1995**, *28*, 1246.
(12) Sutjianto, A.; Curtiss, L. A. *J. Phys. Chem. A* **1998**, *102*, 968.
(13) Johansson, P.; Tegenfeldt, J.; Lindgren, J. *Polymer* **1999**, *40*, 4399.
(14) Rhodes, C. P.; Khan, M.; Frech, R. *J. Phys. Chem. B* **2001**, *106*, 10330.
(15) Dick, C. R.; Ham, G. E. *J. Macromol. Sci., Chem.* **1970**, *A4*, 1301.
(16) Jones, G. D.; MacWilliams, D. C.; Braxtor, N. A. *J. Org. Chem.* **1965**, *30*, 1994.
(17) Harris, C. S.; Ratner, M. A.; Shriver, D. F. *J. Am. Chem. Soc.* **1987**, *109*, 1778.
(18) Paul, J.-L.; Jegat, C.; Lassègues, J.-C. *Electrochim. Acta* **1992**, *37*, 1623.
(19) Sanders, R. A.; Frech, R.; Khan, M. A. *J. Phys. Chem. B* **2004**, *108*, 2186.
(20) *CRC Handbook of Chemistry and Physics*, 70th ed.; CRC Press: Boca Raton, FL, 1989−1990.
(21) Sanders, R. A.; Frech, R.; Khan, M. A. *J. Phys. Chem. B* **2003**, *107*, 8310.

(22) Sanders, R. A.; Frech, R.; Khan, M. A. *J. Phys. Chem. B* **2004**, *108*, 12729.

(23) York, S. S. Oklahoma Baptist University, Shawnee, OK. Rocher, N. M.; Frech, R.; Khan, M. University of Oklahoma, Norman, OK. To be submitted for publication.

(24) Rocher, N. M.; Frech, R.; Khan, M. University of Oklahoma, Norman, OK. To be submitted for publication.

(25) Colthup, N. B.; Daly, L. H.; Wiberley, S. E. *Introduction to Infrared and Raman Spectroscopy*, 3rd ed.; Academic Press: San Diego, CA, 1990.

(26) Pimental, G. C.; McClellan, A. L. *The Hydrogen Bond*; W. H. Freeman: San Francisco, CA, 1960.

(27) Bellamy, L. J.; Williams, R. L. *Spectrochim. Acta* **1957**, *9*, 341.

(28) Wolff, H.; Gamer, G. *J. Phys. Chem.* **1972**, *76*, 871.

(29) Boesh, S.; Wheeler, R. University of Oklahoma, Norman, OK. Calculation of *N*,*N*-DMEDA, *N*,*N*-DMEDA−LiTf, and *N*,*N*-DMEDA−NaTf was performed using B3LYP, a hybrid Hartree−Fock density functional method, with a basis set of 6-31G(d). Unpublished work, 2005.

(30) Rocher, N. M.; Frech, R.; Khan, M. A. *J. Phys. Chem. B* **2005**, *109*, 20697.

(31) Fateley, W. G.; Dollish, F. R.; McDevitt, N. T.; Bentley, F. F. *Infrared and Raman Selection Rules for Molecular and Lattice Vibrations: The Correlation Method*; John Wiley & Sons: New York, 1972.